

## Neutron Density Distributions Deduced from Antiprotonic Atoms

A. Trzcińska, J. Jastrzębski, and P. Lubiński

*Heavy Ion Laboratory, Warsaw University, PL-02-093 Warsaw, Poland*

F.J. Hartmann, R. Schmidt, and T. von Egidy

*Physik-Department, Technische Universität München, D-85747 Garching, Germany*

B. Kłos

*Physics Department, Silesian University, PL-40-007 Katowice, Poland*

(Received 28 March 2001; published 2 August 2001)

The differences between neutron and proton density distributions at large nuclear radii in stable nuclei were determined. Two experimental methods were applied: nuclear spectroscopy analysis of the antiproton annihilation residues one mass unit lighter than the target mass and the measurements of strong-interaction effects on antiprotonic x rays. Assuming the validity of two-parameter Fermi neutron and proton distributions at these large radii, the conclusions are that the two experiments are consistent with each other and that for neutron rich nuclei it is mostly the neutron diffuseness which increases and not the half-density radius. The obtained neutron and proton rms radii differences are in agreement with previous results.

DOI: 10.1103/PhysRevLett.87.082501

PACS numbers: 21.10.Gv, 13.75.Cs, 36.10.-k

The fact that the proton and neutron distributions may not be exactly the same at the surface of stable nuclei was recognized already at the very beginning of contemporary nuclear physics (see Ref. [1]). Their differences, studied experimentally [2,3] and theoretically [4–6] for decades, are pursued today [7,8] and new, often sophisticated experiments are proposed [9]. This is, on the one hand, motivated by the fact that the shapes and sizes are among the fundamental properties of atomic nuclei. On the other hand, large differences between neutron and proton radii are expected [10] to characterize the nuclei at the border of the stability line, the future domain of nuclear structure studies. Therefore, the information on these quantities for stable nuclei is a convenient starting point for studies of more exotic nuclei.

Experimental information on the radial neutron distribution is generally obtained by measuring its mean square radius [3,11,12] or determining the difference  $\Delta r_{np}$  between the neutron and proton mean square radii [13]. It is believed that the proton radii and a few higher moments of their distribution are well known from charge sensitive experiments [3]. Much less is known about higher moments of the peripheral neutron distributions [3,11] in stable nuclei. Surprisingly, in spite of the lack of experimental evidence these distributions are often assumed to form a “neutron skin.” Unfortunately, besides some exceptions [14,15], the precise definition of this term is often not given in the literature. Remaining within simple two-parameter Fermi (2pF) distributions of the neutron and proton peripheral density, the “neutron skin-type” distribution will be understood in this Letter as having a neutron half-density radius  $c_n$  which is larger than the proton half-density radius  $c_p$ , and equal diffuseness parameters  $a_n = a_p$ . The other extreme  $c_n = c_p$  and  $a_n > a_p$  will be

called “neutron halo-type” distribution. Intermediate, less well-defined distributions for which  $c_n > c_p$  and  $a_n > a_p$  are, naturally, also possible.

Already more than a quarter of a century ago it was recognized [16–18] that, thanks to the strong hadron-nucleon interaction, the study of hadronic atom observables can provide information on the extent and composition of the outer nuclear periphery. However, besides a few analyses of the characteristic x-ray spectra of these atoms [19–21], systematic investigations aiming at the determination of the properties of the nuclear periphery [22,23] are scarce.

Eight years ago, we started a program of nuclear periphery studies using antiprotons from the late Low Energy Antiproton Ring at CERN. First, we proposed a new, conceptually simple and experimentally easy way to determine the peripheral neutron to proton density ratio using a radiochemical method [24]. Next, we supplemented the radiochemical data [25–27] by a series of in-beam antiprotonic x-ray studies [28] determining strong-interaction level widths and shifts in a number of isotopically enriched targets.

As calculations indicate [29], both methods test the outer part of the nuclear periphery in quite different although partly overlapping regions. Therefore their application to the same target nuclei should, in principle, substantially constrain the deduced parameters of the peripheral neutron distribution (assuming again that the charge or proton distributions are known from charge sensitive experiments). In this Letter, after a short reminder of the principle of the radiochemical method, we first conclude on the type (“skin” or “halo”) of peripheral neutron distribution deduced from these experiments. Next, referring to the recently reported x-ray data [28], we compare both methods probing the nuclear periphery at large radial distances

and, assuming 2pF distributions, extrapolate the deduced densities towards the interior of the nucleus. This allows us to calculate the differences between such determined rms neutron and proton radii and to compare them with results from other methods measuring this quantity.

The radiochemical method consists of the study of the annihilation residues with mass number one unit smaller than the target mass  $A_t$ . These products originate from annihilation events in which all produced pions miss the nucleus, leaving it at such a low excitation energy that evaporation or fission does not occur. When both  $A_t - 1$  products (i.e., those with proton number  $Z_t - 1$  and those with neutron number  $N_t - 1$ ) are radioactive, their relative yields after antiproton annihilation are easily determined by standard nuclear-spectroscopy methods. These yields are directly related to the proton and neutron densities at the annihilation site. The radial distance of this site, almost independent of the atomic number  $Z$  of the target is obtained from calculations [29] making use of the available antiproton-nucleus optical potential and antiprotonic orbits involved in the annihilation process. The calculations indicate that the annihilations leading to the  $A_t - 1$  products are localized at distances about 2.5 fm larger than the half-density charge radius  $c$ . The width of the annihilation probability distribution for events testing the density ratio is between 2 and 3 fm (see Fig. 10 of Ref. [26]).

Using this method the composition of the nuclear periphery was investigated for 19 medium- and heavy-mass nuclei. It was shown that, in the heavy isotopes of a given element, this periphery is largely composed of neutrons. To describe the observed phenomenon in a quantitative way the “halo factor” was introduced, following the definition proposed previously [18]. This halo factor is defined as

$$f_{\text{halo}} = \frac{N(\bar{p}n)}{N(\bar{p}p)} \frac{Z}{N} \frac{\text{Im}a(\bar{p}p)}{\text{Im}a(\bar{p}n)},$$

where the first term gives the ratio of annihilations on peripheral neutrons to those on peripheral protons (close to the ratio of produced nuclei with  $N_t - 1$  to those with  $Z_t - 1$ ). The second term normalizes this annihilation ratio with the target  $Z/N$  value. The third term, the ratio of the imaginary parts of the antiproton-nucleon scattering amplitudes, expresses the ratio of the annihilation probability on a proton to that on a neutron.

In all our previous publications on the results and analyses of the radiochemical experiments we have assumed, in agreement with previously published values [18,30], that the ratio  $R = \text{Im}a(\bar{p}n)/\text{Im}a(\bar{p}p)$  is equal to 0.63. However, the comparison of the results from the x-ray method discussed below with the radiochemical method clearly favors, for most of the cases studied, a larger value of this ratio, close to 1, in agreement with all simple, phenomenological antiproton-nucleon optical potentials proposed earlier [31] and recently [32,33]. Therefore, in what

follows, the value  $R = 1$  will be used, although this assumption leads to the somewhat curious result of a proton rich nuclear periphery in the investigated lightest members of some isotopic chains:  $^{96}\text{Ru}$ ,  $^{106}\text{Cd}$ ,  $^{112}\text{Sn}$ , and  $^{144}\text{Sm}$ . This anomaly seems, however, to be explained [33].

The halo factor defined above expresses the normalized neutron to proton density ratio  $\rho_n/\rho_p$  integrated over the whole interaction region leading to events producing  $A_t - 1$  nuclei. For the purpose of presentation we assume here that the  $f_{\text{halo}}$  factor corresponds to the  $Z/N\rho_n/\rho_p$  value at a radial distance equal to the (calculated) most probable annihilation site. We have verified for several cases that such a simplified presentation does not introduce errors larger than 10%–15%.

As an example, in Fig. 1 we present for three nuclei with large neutron excess the experimentally determined halo factor at the radial distance of  $c_{ch} + 2.5$  fm (where  $c_{ch}$  is the half-density charge radius), i.e., at the most probable annihilation site for events leading to  $A_t - 1$  products. In the same figure we also show the normalized neutron to proton density ratios deduced from recent [7,11,13,36] or older [34,35,37] experiments, determining the  $\Delta r_{np}$  values directly. In preparing this figure the experimentally determined  $\Delta r_{np}$  values were first used to obtain the neutron rms radius from the relation  $\langle r_n^2(c_n, a_n) \rangle^{1/2} = \langle r_p^2(c_p, a_p) \rangle^{1/2} + \Delta r_{np}$ , where  $\langle r_p^2 \rangle^{1/2}$  was taken from the recent tabulation [38] after correcting for the proton charge radius. The same tabulation gives the 2pF charge distributions. These distributions were converted to point proton distributions [39]. The parameters for the bare neutron distributions were obtained from the relation  $\langle r_n^2 \rangle \approx \frac{3}{5}c_n^2 + \frac{7}{5}\pi^2 a_n^2$  assuming either  $c_n = c_p$  or  $a_n = a_p$ . These two cases are shown in Fig. 1. As can be seen from this figure our radiochemical data are clearly in favor of interpreting  $\Delta r_{np}$  as an increase of the neutron surface diffuseness rather than an increase of the neutron half-density radius. However, within assigned errors, some room is left for the intermediate cases with

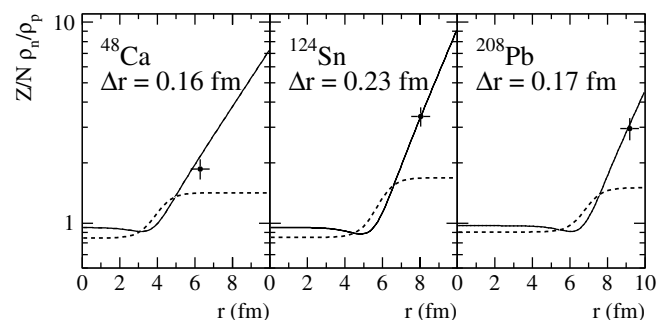


FIG. 1. Normalized neutron to proton density ratios  $\frac{Z}{N} \frac{\rho_n}{\rho_p}$  deduced from the previously determined experimental  $\Delta r_{np}$  values for  $^{48}\text{Ca}$  [34–36],  $^{124}\text{Sn}$  [7,13,34],  $^{208}\text{Pb}$  [11,37]. Crosses indicate the density ratio deduced from our radiochemical experiments (interpolated value for  $^{208}\text{Pb}$ ) presented at the most probable annihilation site. Solid line:  $c_n = c_p$  (“neutron halo” model), dashed line:  $a_n = a_p$  (“neutron skin” model).

$c_n > c_p$  and  $a_n > a_p$ . A similar conclusion was reached from the analysis of kaonic atoms in Ref. [21].

Another set of observables, the strong interaction widths and shifts of antiprotonic atom levels, is sensitive to the properties of the nuclear periphery at distances about 1 fm closer to the nuclear center [29] than the halo factors. In Ref. [28] the experimentally determined level shifts and widths were reported for 34 monoisotopic or isotopically separated targets ranging from  $^{16}\text{O}$  to  $^{238}\text{U}$ . In the present work, the neutron distributions were obtained from these x-ray data, assuming again 2pF parametrization for protons and neutrons and an antiproton-nucleon scattering length of the form  $\bar{a} = (2.5 \pm 0.3) + i(3.4 \pm 0.3)$  fm as proposed for pointlike nucleons in Ref. [32]. Bare proton distributions were obtained from tabulated charge distributions in the way indicated above. The half-density radii of the proton and neutron distributions were assumed to be equal  $c_n = c_p$ , in agreement with the analysis of the radiochemical data. The difference  $\Delta a_{np}$  between neutron and proton diffuseness was adjusted to account best for the lower and upper level widths and the lower level shift. Figure 2 gives examples of the comparison of the normalized neutron to proton density ratio deduced from the x-ray data with the same ratio obtained from the Hartree-Fock-Bogoliubow (HFB) model [40] and the halo factor previously discussed. For the  $R = 1$  value adopted here fair agreement between the two experimental approaches and the model calculations is observed.

The next objective of the present Letter is the comparison of the neutron and proton distribution rms radius differences  $\Delta r_{np}$  obtained from the analysis of antiprotonic atom data and from other methods [2,3,7,11,13,36]. An example is presented in Fig. 3, still under the assumption that the 2pF proton and neutron distributions are valid for radial distances extending from about the nuclear rms radius to distances about 3.5 fm larger. Again, the agreement between antiprotonic data and other methods is satisfactory.

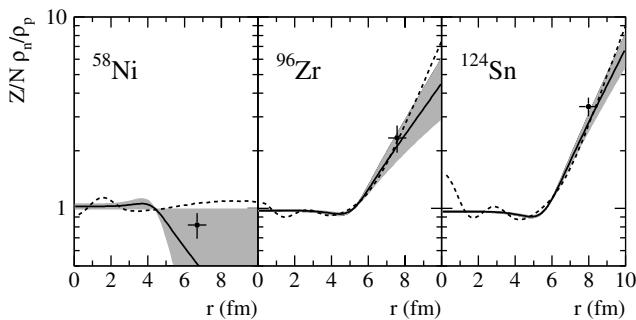


FIG. 2. Normalized neutron to proton density ratios  $\frac{Z}{N} \frac{\rho_n}{\rho_p}$  deduced from strong-interaction level widths and shifts (solid lines with indicated statistical error) and charge distributions given in Refs. [38,41], for  $^{58}\text{Ni}$ ,  $^{96}\text{Zr}$ , and  $^{124}\text{Sn}$ , respectively. They are compared with  $f_{\text{halo}}$  measured in the radiochemical experiments (marked with crosses at a radial distance corresponding to the most probable annihilation site) and with HFB model calculations [40] (dashed lines).

Finally, following the presentation proposed in Ref. [14], Fig. 4 gives all determined differences between rms radii of the neutron and the proton distributions as a function of the asymmetry parameter  $\delta = (N - Z)/A$ . Although in a number of analyzed cases the statistical errors are rather large, the linear relationship between  $\Delta r_{np}$  and the asymmetry parameter seems to emerge from the data of Fig. 4. Assuming such a dependence, the fitted relationship is  $\Delta r_{np} = (-0.04 \pm 0.03) + (1.01 \pm 0.15)\delta$  fm with  $\chi^2$  of 0.6.

At this point let us comment on three  $\Delta r_{np}$  values, recently discussed [8] in relation to the neutron equation of state (EOS). It was shown that from 18 Skyrme parameter sets used in the Hartree-Fock model the SkX parametrization fulfills the constraints imposed by the neutron EOS, i.e.,  $\Delta r_{np}(^{208}\text{Pb}) = 0.16 \pm 0.02$  fm. Moreover, the same parametrization leads to  $\Delta r_{np}(^{138}\text{Ba}) = 0.15$  fm and  $\Delta r_{np}(^{132}\text{Sn}) = 0.22$  fm. The weighted average of previous values for  $\Delta r_{np}(^{208}\text{Pb})$  is  $0.17 \pm 0.03$  fm (cf. Fig. 1). Our experimental result is  $\Delta r_{np} = 0.15 \pm 0.02$  fm, whereas the interpolated value, taking into account all antiprotonic data, would be  $0.18 \pm 0.03$  fm. Finally, the interpolated or extrapolated values for  $^{138}\text{Ba}$  and  $^{132}\text{Sn}$  are  $0.15 \pm 0.03$  fm and  $0.21 \pm 0.04$  fm, respectively.

In conclusion, in this Letter we have presented information on the neutron distributions in stable nuclei deduced from the antiprotonic atom observables under the assumption that the proton distributions are well known from charge sensitive experiments. The radiochemical

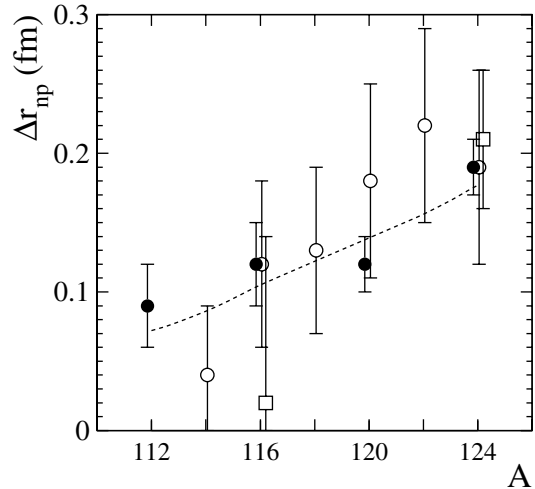


FIG. 3. Comparison of the  $\Delta r_{np}$  values for Sn isotopes calculated with the parameters of the neutron distribution obtained from x-ray data (full circles) with those obtained from the ( $^3\text{He}, t$ ) reaction [7] (open circles) and inelastic  $\alpha$  scattering [13] (open squares). The prediction of HFB model calculation with the Skyrme (SLy4) force [5] is also drawn (dashed line). The 2pF proton distributions were deduced from charge distributions of Ref. [41]. Only statistical errors are given for the antiprotonic data.

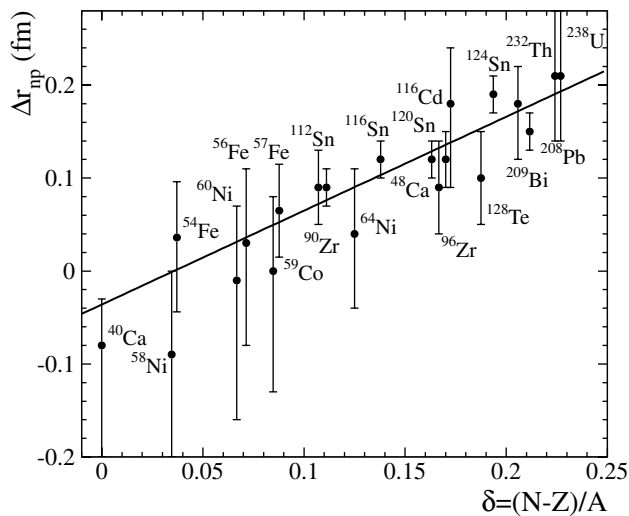


FIG. 4. Difference  $\Delta r_{np}$  between the rms radii of the neutron and proton distributions as deduced from the antiprotonic atom x-ray data, as a function of  $\delta = (N - Z)/A$ . The proton distributions were obtained from electron scattering data [41] (Sn nuclei) or from muonic atom data [38,42,43] (other nuclei). The full line represents the linear relationship between  $\delta$  and  $\Delta r_{np}$  as obtained from a fit to the experimental data.

results clearly favor the peripheral neutron distribution in the form of a neutron halo rather than a neutron skin. This observation constrains the neutron distribution parameters deduced from the analysis of the strong-interaction level widths and shifts, leaving only the difference between neutron and proton diffuseness as a free parameter. Under the assumption of an identical antiproton-neutron and antiproton-proton scattering length, fair agreement between radiochemical and x-ray data was obtained. Reasonable agreement is also obtained between the  $\Delta r_{np}$  values deduced from the antiprotonic x-ray data and those measured using various other methods. All these findings indicate that the assumption of the simplest, i.e., the two-parameter Fermi, proton, and neutron peripheral distributions are adequate, at least for the degree of precision of the experiments described in this Letter.

We thank all members of the PS209 team for their participation in the experiments and for discussions. Our thanks are due to Sławomir Wycech for help and criticism and to Jacek Dobaczewski for commenting on this manuscript. This work was supported by KBN Grants No. 2P03B 048 15 and No. 2P03B 119 16 and by the Deutsche Forschungsgemeinschaft, Bonn.

[1] R. C. Barrett and D. F. Jackson, *Nuclear Sizes and Structure* (Clarendon Press, Oxford, 1980).

- [2] A. Chaumeaux, V. Layly, and R. Schaeffer, *Ann. Phys. (N.Y.)* **116**, 247 (1978).
- [3] C. J. Batty *et al.*, in *Advances in Nuclear Physics*, edited by J. W. Negele and E. Vogt (Plenum Press, New York, 1989), Vol. 19, p. 1.
- [4] J. W. Negele, *Phys. Rev. C* **1**, 1260 (1970).
- [5] F. Hofmann and H. Lenske, *Phys. Rev. C* **57**, 2281 (1998).
- [6] K. Pomorski *et al.*, *Nucl. Phys.* **A624**, 349 (1997).
- [7] A. Krasznahorkay *et al.*, *Phys. Rev. Lett.* **82**, 3216 (1999).
- [8] B. A. Brown, *Phys. Rev. Lett.* **85**, 5296 (2000).
- [9] C. J. Horowitz *et al.*, *Phys. Rev. C* **63**, 025501 (2001).
- [10] J. Dobaczewski, W. Nazarewicz, and T. R. Werner, *Z. Phys. A* **354**, 27 (1996).
- [11] V. E. Starodubsky and N. M. Hintz, *Phys. Rev. C* **49**, 2118 (1994).
- [12] T. Suzuki *et al.*, *Phys. Rev. Lett.* **75**, 3241 (1995).
- [13] A. Krasznahorkay *et al.*, *Nucl. Phys.* **A567**, 521 (1994).
- [14] C. J. Pethick and D. G. Ravenhall, *Nucl. Phys.* **A606**, 173 (1996).
- [15] S. Mizutori *et al.*, *Phys. Rev. C* **61**, 044326 (2000).
- [16] D. H. Wilkinson, *Philos. Mag.* **4**, 215 (1959).
- [17] D. H. Davis *et al.*, *Nucl. Phys.* **B1**, 434 (1967).
- [18] W. M. Bugg *et al.*, *Phys. Rev. Lett.* **31**, 475 (1973).
- [19] C. J. Batty *et al.*, *Phys. Lett.* **81B**, 165 (1979).
- [20] R. J. Powers *et al.*, *Nucl. Phys.* **A336**, 475 (1980).
- [21] C. J. Batty *et al.*, *Phys. Rev. C* **40**, 2154 (1989).
- [22] R. Kunselman *et al.*, *Nucl. Phys.* **A405**, 627 (1973).
- [23] C. Garcia-Recio, J. Nieves, and E. Oset, *Nucl. Phys.* **A547**, 473 (1992).
- [24] J. Jastrzębski *et al.*, *Nucl. Phys.* **A558**, 405c (1993).
- [25] P. Lubiński *et al.*, *Phys. Rev. Lett.* **73**, 3199 (1994).
- [26] P. Lubiński *et al.*, *Phys. Rev. C* **57**, 2962 (1998).
- [27] R. Schmidt *et al.*, *Phys. Rev. C* **58**, 3195 (1998).
- [28] A. Trzcińska *et al.*, in *Proceedings of the Sixth Biennial Conference on Low-Energy Antiproton Physics, Venice, 2000* (to be published) (nucl-ex/0103008).
- [29] S. Wycech *et al.*, *Phys. Rev. C* **54**, 1832 (1996).
- [30] M. Wade and V. G. Ling, *Phys. Rev. A* **9**, 1182 (1976).
- [31] C. J. Batty, *Nucl. Phys.* **A372**, 433 (1981).
- [32] C. J. Batty, E. Friedman, and A. Gal, *Nucl. Phys.* **A592**, 487 (1995).
- [33] S. Wycech, in *Proceedings of the Sixth Biennial Conference on Low-Energy Antiproton Physics, Venice, 2000* (to be published) (nucl-th/0012053).
- [34] L. Ray, *Phys. Rev. C* **19**, 1855 (1979).
- [35] H. J. Gils, H. Rebel, and E. Friedman, *Phys. Rev. C* **29**, 1295 (1984).
- [36] W. R. Gibbs and J. P. Dedonder, *Phys. Rev. C* **46**, 1825 (1992).
- [37] G. W. Hoffman *et al.*, *Phys. Rev. C* **21**, 1488 (1980).
- [38] G. Fricke *et al.*, *At. Data Nucl. Data Tables* **60**, 177 (1995).
- [39] E. Oset *et al.*, *Phys. Rep.* **188**, 79 (1990).
- [40] R. Smolańczuk (private communication).
- [41] H. de Vries, C. W. de Jager, and C. de Vries, *At. Data Nucl. Data Tables* **36**, 495 (1987).
- [42] J. D. Zumbro *et al.*, *Phys. Rev. Lett.* **20**, 1888 (1984).
- [43] J. D. Zumbro *et al.*, *Phys. Lett.* **167B**, 383 (1986).